INL/JOU-15-34249
Accepted Manuscript

Experimental Design, Operation, and Results of a 4 kW High Temperature Steam Electrolysis Experiment

Xiaoyu Zhang, James E. O'Brien,
Can Zhou, Gregory K. Housley,
Greg Tao

November 2015

The INL is a
U.S. Department of Energy
National Laboratory
operated by
Battelle Energy Alliance

This is an accepted manuscript of a paper intended for publication in a journal. This document was prepared as an account of work sponsored by an agency of the United States Government. Neither the United States Government nor any agency thereof, or any of their employees, makes any warranty, expressed or implied, or assumes any legal liability or responsibility for any third party's use, or the results of such use, of any information, apparatus, product or process disclosed in this report, or represents that its use by such third party would not infringe privately owned rights. The views expressed in this paper are not necessarily those of the United States Government or the sponsoring agency.

Prepared for the U.S. Department of Energy
Office of Nuclear Energy
Under DOE Idaho Operations Office
Contract DE-AC07-05ID14517

Experimental Design, Operation, and Results of a 4 kW High Temperature Steam Electrolysis Experiment

Xiaoyu Zhang [a, *], James E. O'Brien [b], Can Zhou [a], Gregory K. Housley [b], Greg Tao [c]

[a] Department of Mechanical & Aerospace Engineering, Old Dominion University, Norfolk, VA 23529, USA

[b] Idaho National Laboratory, Idaho Falls, ID 83401, USA

[c] Materials and Systems Research, Inc., Salt Lake City, UT 84104, USA

* *Corresponding author. Kaufman Hall 238, Old Dominion University, Norfolk, VA 23529, USA. Tel.: +1 757-683-4913; fax: +1 757-683-5344. E-mail: x1zhang@odu.edu.*

Abstract

High temperature steam electrolysis (HTSE) is a promising technology for large-scale hydrogen production. However, research on HTSE performance above the kW level is limited. This paper presents the results of 4 kW HTSE long-term test completed in a multi-kW test facility recently developed at the Idaho National Laboratory (INL). The 4 kW HTSE unit included two solid oxide electrolysis stacks operating in parallel, each of which included 40 electrode-supported planar cells. A current density of 0.41 A/cm^2 was used for the long-term operation, resulting in a hydrogen production rate about 25 slpm. A demonstration of 920 hours stable operation was achieved. The paper also includes detailed descriptions of the piping layout, steam generation and delivery system, test fixture, heat recuperation system, hot zone, instrumentation, and operating conditions. This successful demonstration of multi-kW scale HTSE unit will help to advance the technology toward near-term commercialization.

Key words: High Temperature Steam Electrolysis, Solid Oxide Electrolysis Cell, Hydrogen Production, Multi-kW Test

Highlights

- Designed and built the test facility for muti-kW scale high temperature steam electrolysis (HTSE).
- Provided design factors and development details for muti-kW scale HTSE tests.
- Demonstrated long-term stable operation of a 4 kW HSTE unit with 80 SOECs.

1 Introduction

Hydrogen is a potentially renewable fuel that can help meet the rapidly growing global energy demand. However, hydrogen is not a direct energy source. It is an energy carrier that must be produced from other energy resources such as fossil fuels [1], nuclear, solar, biomass, etc. Currently, hydrogen production is mainly dependent on steam reforming of methane. However, from a long-term perspective, hydrogen needs to be produced from sustainable resources. High temperature steam electrolysis (HTSE) has emerged as a promising technology for large-scale sustainable hydrogen production (> 500,000 kg/day) [2]. Large-scale hydrogen production using HTSE coupled with the next generation nuclear plant (NGNP) was selected as the leading candidate by the United States Department of Energy (DOE) as the leading candidate for carbon-free nuclear hydrogen production research and development (R&D) [3].

The HTSE process consumes electricity as well as heat, and is highly efficient. In terms of thermodynamics [4], the electrical energy requirement decreases while the thermal energy requirement increases with increasing temperature. The total energy requirement is nearly constant. Therefore, at elevated temperature (e.g. 800 °C), a large part of electricity input can be substituted by heat, leading to higher efficiency. Meanwhile, several restraining factors, e.g. activation, kinetics and ohmic overpotentials decrease remarkably with rising temperature [5]. When powered by a high-temperature nuclear reactor system, HTSE has the potential to achieve 50% [6] or even higher overall thermal-to-hydrogen efficiency. based on higher heating value (HHV). Furthermore, according to a life cycle assessment (LCA) [7], the global warming potential (GWP) and acidification potential (AP) of HTSE process are one sixth and one-third, respectively, of those for hydrogen production by steam reforming of natural gas, and are competitive compared with conventional electrolysis powered by renewable energy.

The history of HTSE is related to the R&D of the solid oxide fuel cell (SOFC). Back in 1980s, Doenitz and his German co-workers in 'Hot Elly' project published that the thermal efficiency of electrolytic hydrogen production can be as high as 40-50% when operating with water in the vapor phase [8]. Due to shorter sealing lengths and simpler fabrication technology, a serial tubular configuration was chosen initially as the single cell for scaling up the design [9]. Subsequently, electrolysis units for modular integration were developed and tested successfully with respect to electricity consumption of 2.57 kWh/Nm^3 (H_2) [10]. Additionally, a 21.6 W tube stack assembled by 10 series-connected cells was used to investigate the viability of high H_2 concentration at the outlet [10]. At the end of that project, the concepts of prototype plant with 3.5 kW hydrogen output power were proposed [11]. After that, the worldwide focus of solid-oxide R&D moved to SOFCs, which had gone through an impressive progress in recent two decades. Recently, energy supply and global warming concerns have renewed the research on HTSE using advanced technologies of solid-oxide cells.

There has been a growing interest globally on R&D of HTSE stacks for producing hydrogen as well as syngas in the past decade. The Idaho National Laboratory (INL) focused on the feasibility of using SOECs for large-scale hydrogen and syngas production [1, 12]. Both experimental investigations (single button cell tests, multi-cell stacks, and multi-stack systems) [13, 14] and computational simulations (1-D and 3-D) [15] were performed. In European Institute for Energy Research (EIFER), numerous experiments of HTSE stacks with test durations ranging from 1000 to 9000 hours were reported [16]. Researchers in Denmark used 6-cell and 10-cell stacks to investigate HTSE and co-electrolysis of steam and CO_2, respectively. The results showed that absorption of impurities from inlet gas played a major role in polarization resistance degradation of stacks [17]. Aimed at improving performance and reducing

cost, A French group in Alternative Energies and Atomic Energy Commission (CEA) designed a 3-cell short stack using thin interconnects. They achieved mitigation of the degradation rate below 3%/1000 h [18, 19]. Institute of Nuclear and New Energy Technology (INET) in China has started R&D of hydrogen production using HTSE coupled with High Temperature Gas-cooled Reactor (HTGR), similar to work performed under the DOE NGNP program in the U.S. [20, 21]. In addition, optimization tests of a 30-cell HTSE stack were conducted in Ningbo Institute of Materials Technology and Engineering (NIMTE) in China. They achieved a maximum hydrogen production rate of 103.6 NL/h and a system efficiency of 52.7% [22, 23]. Researchers in Korea Institute of Energy Research investigated a 3-cell HTSE stack prepared by extrusion method, and confirmed that sufficient steam supply was feasible to facilitate water splitting and decrease activation energy [24]. Another group from Korea Institute of Science and Technology (KIST) tested a 200 W class solid oxide regenerative fuel cell (SORFC) stack. A degradation rate of 7.75%/1000 h was observed when the stack was operated in the electrolysis mode [25].

Although many HTSE stack tests have been reported, most of them are constrained below the kW level. To demonstrate the feasibility of commercialization of this technology, more large-scale (kW and above) tests need to be conducted. To our best knowledge, only a couple of groups performed HTSE stack tests in multi-kW scale. EIFER researchers reported a 25-cell stack (≥ 2 kW) with more than 2900 h continuous operation in electrolysis mode in 2012. The objective of the long-term test was to identify the mechanisms leading to degradation of cells and stacks performance [16]. INL developed a 15 kW Integrated Laboratory Scale (ILS) HTSE experimental facility to investigate performance and degradation of steam electrolysis process back in 2009 [13] . The ILS system consisted of three modules (each module consists of 240

SOECs) and was tested for 1080h with hydrogen production rate about 1.2 Nm^3/hr. However, significant degradation was observed during the test.

This paper reports results of a durable 4 kW HTSE stack test with more advanced electrode-supported SOECs. A new stack test facility for multi-kW scale HSTE was designed and built at INL for this test. Long-term operation (920 hours) of a 4 kW HTSE stack with 80 SOECs was demonstrated. This test demonstrated a low degradation rate due to R&D improvements of SOECs.

2 Experimental

2.1 Experimental design

Designing multi-kW HTSE tests is not a simple scaling-up process of single cell or short stack tests. Compared to small scale tests, as the power and heating demand, and gas flow rates significantly increase, multi-kW tests require modification or even redesign on many apparatus components. Table I lists the common design factors that need to be considered for multi-kW tests and the specifications used in this research.

The 4 kW HTSE experimental process is illustrated in a piping and instrumentation diagram (P&ID) presented in Figure 1. The P&ID shows the double SOEC stacks inside the furnace with supporting instrumentation, including mass-flow controllers (MFCs), steam generator, heat exchangers, dew point sensors, thermocouples, and pressure transducers. In a standard long-term test (1000 hours), the feedstock to the cathode side consists of water vapor produced by a steam generator and carrier gases (H_2 or H_2+N_2). The dew point sensors are used to measure the steam content in the inlet and outlet streams so that the H_2 production rate can be calculated independently, as compared to the data obtained from the current measurement. On the anode side, produced O_2 is purged with a sweep gas (N_2 or air). The SOEC stacks are located inside of a cylindrical clamshell ceramic-fiber furnace. The inlet gases are preheated

before entering the furnace through heat recuperation from the hot outlet gases. The gases are heated to the final 800°C operating temperature within the furnace by means of radiant heating. The inlet gases flow through coiled tubing inside the furnace upstream of the stack for this purpose. All the outlet gases are vented outside the building.

For the 4 kW long-term tests, a mixture of hydrogen, nitrogen, and steam is introduced to the cathode side of the electrolysis cells. Hydrogen is required on the inlet side in order to maintain reducing conditions on the nickel cermet electrode of the SOECs. Inlet hydrogen for these tests is supplied by a pressurized, low-temperature water electrolysis unit (Avalence LLC) at 6 slpm with additional hydrogen from compressed gas cylinders at 6 slpm. Nitrogen is included in the cathode gas mixture to yield a total dry gas mole fraction of 30% with a hydrogen mole fraction of 17%. The inclusion of nitrogen reduces the required inlet hydrogen flow rate to a value that could be supported by the electrolyzer unit and the available mass flow controllers. Air or nitrogen flows across the anode side of the electrolysis cells as a sweep gas. Nitrogen is supplied by two cryogenic Dewars. Air is supplied using a shop air compressor at 50 slpm.

Steam is provided by an electrically heated steam generator. The steam generator includes two independently heated zones. The lower boiling zone is controlled at constant power, with the power value depending on the required steam production rate. The rate of steam production for these tests yields an inlet steam mole fraction of 70%. The upper zone is feedback-controlled on temperature in the single-phase steam region above the liquid. The two-zone strategy allows for steady steam production with a desired amount of superheat. The gas flow lines downstream of the steam generator are heat-traced to avoid condensation. The outlet gas flow mixture flows through a water-cooled condenser, where the majority of the residual steam is condensed, and then to the roof vent.

Stack power is provided by a 10 kW DC power supply rated at 100 V and 100 A. Nominal electrolysis power consumption during operation is 4.2 kW at 30 A and 70 V. The stacks are instrumented with intermediate voltage taps on every eight cells.

The hydrogen/nitrogen inlet gas flow is mixed with steam downstream of the steam generator. After mixing, the dew point temperature of the resulting steam/hydrogen/nitrogen mixture is measured using a precision dew point sensor. Another dew point sensor is located downstream of the SOEC stacks. The two dew point measurements provide an independent direct measurement of the steam consumption rate in the SOEC stacks, which is equal to the hydrogen production rate on a molar basis.

2.2 Test stand

The 4 kW test stand is shown in Figure 2. A rendering of the 3-D CAD design is shown in Figure 2a and a photograph of the completed assembled test stand is shown in Figure 2b. A split-tube furnace (40.6 cm ID × 54.3 cm height) is vertically mounted on a supporting shaft. The split-tube design provides convenient access during assembly and maintenance of test articles without physically removing the furnace. The furnace has an electrical power rating up to 15 kW and can be operated at temperatures up to 1000 ºC.

The rendering in Figure 2a is labeled to show the top current collector rods, springs for stack compression, alumina load transfer tubes, furnace, SOEC stacks, base manifold plate, and recuperative heat exchangers. The base manifold plate is supported by an alumina tube, which acts as an electrical insulator as well. The stacks are shown in their uncompressed state. After conditioning and final compression, the height of the stacks is significantly reduced.

The test fixture is based on a design developed at MSRI for smaller scale tests. The compression apparatus is capable of providing compressive force to the top of a stack during testing via compression springs located outside the hot zone of the furnace. A total compression load of 1.775 kN per stack is used. The compression load is transferred to the stack via an alumina load transfer tube and the upper electrode plates as shown in Figure 2. Once the stack is in place on the test fixture, alumina load transfer tubes are installed on top of the upper electrodes, onto which compression springs with pusher plates are placed. Compression of the stack to the desired loading is achieved by tightening nuts on the four threaded bars

that stand in parallel to each load transfer tube and fixed to the lower test fixture portion running through the pusher plates. Upon achieving the desired initial compression of the springs and hence, forced loading of the stack, the furnace may be closed and a heatup procedure is executed. During heatup, spring compression is monitored and carefully adjusted to maintain the prescribed load to compensate for thermal expansion of the threaded rods and compression of the compliant seals in the stack.

A custom base manifold plate was designed and fabricated for the double-stack configuration. The plate provides mechanical support for the two SOEC stacks, serves as a bottom current collector, and distributes the inlet and outlet gas flows to and from the double stacks. Detailed views of the base manifold plate made of Inconel 625 are provided in Figure 3. Figure 3a is a top view showing the four flow channels (two inlets and two outlets) that mate with corresponding flow channels in each stack. Figure 3b is the bottom view showing the gas inlet and outlet tubing welded to the plate. There are only two gas inlet lines and two gas outlet lines on the underside of the manifold plate, whereas there are four inlet channels and four outlet channels on the top side of the manifold plate. The inlet and outlet gas flows are distributed to/from the two stacks by means of flow channels that were milled into the base manifold plate and subsequently seal-welded.

As mentioned above, the base manifold plate serves as a bottom current collector, which electrically commons the bottom sides of two stacks. During operation, the top two current collectors are also connected to the same power terminal, resulting in the same voltage being applied onto both stacks. This arrangement may result in different values of current in the two stacks. A drawback of this configuration is that if one stack endures a catastrophic failure, it will significantly affect the other stack. In practice, a limiting voltage is programed to prevent that instance. As an alternative strategy, independent current controll of the two stacks separately was also evaluated in the initial design. However, independent control was deemed not feasible, due to its requirement of an additional power supply and a more complicated piping arrangement and instrument wiring.

Figure 4 shows a color-coded diagram of the inlet and outlet gas flows and the locations of the seal-welded flow channels. The steam/hydrogen and air sweep gas inlet lines are fed from the coiled tubing, which provides sufficient length for heat transfer from the furnace to the gases to ensure that the gas temperatures reach the desired stack operating temperature of 800°C prior to entering the stack. The outlet gas lines are not coiled.

2.3 SOEC stacks

The SOEC stacks used in this research were manufactured by MSRI. An exploded view of a short MSRI SOEC stack is provided in Figure **5**. The cells incorporate semi-elliptical cut-out gas flow channels (four per side) around the outer periphery of the cells that mate with corresponding holes in the interconnect plates . The stack is internally manifolded with compliant seals. Treated metallic interconnects with integral flow channels separate the cells and electrode gases. The stack operates in cross-flow, with an inverted-U shaped overall flow pattern such that the gas flow inlets and outlets are all located underneath the stack. Stack mechanical compression is accomplished by means of the custom spring-loaded test fixture described previously. The compliant seals are oriented at each level in the stack to allow for gas flow along either the anode or the cathode side of the cells.

The SOECs used for this study have a square profile with outer dimensions of 15.2 × 15.2 cm and a cell active area of 100 cm^2. The cells incorporate an electrode-supported multilayer configuration with nickel-zirconia cermet negative electrodes, thin-film yttria-stabilized zirconia electrolytes, and multilayer lanthanum ferrite-based positive electrodes. The nickel zirconia electrode has a support layer thickness of 700 μm and a graded functional layer with an overall thickness of 15 μm. The electrolyte thickness is 8-10 μm. The positive electrode has a graded functional layer with a thickness of 20 μm and a current collecting layer thickness of 50 μm.

Installation of MSRI stacks within the test section is a relatively simple procedure. Correct alignment of the process gas (steam/H_2) and air inlets and outlets of the stack to the corresponding flow channels of the test section is most critical. Compliant gasket seals are placed underneath and atop of the stack prior

to placement on the test fixture lower electrode/gas distribution plate. Contact aids are used to assist electrical contact between the stack and the upper and lower fixture electrodes.

2.4 Steam generator

For the 4 kW HTSE tests, the inlet steam flow rate will be relatively high (about 50 slpm). Commerical lab-scale steam generators usually are not able to meet the requirement of this research. Therefore, a steam generator was designed and built in house at INL. The custom steam generator shown in Figure 6 consists of a heated vertical tube with two independently heated sections—a lower constant-power boiler section and an upper constant-temperature superheater section. The boiler portion vaporizes the water while the smaller superheater section heats the saturated steam from the boiler to a temperature of about 150°C. It was fabricated by attaching a combination of twenty 200 and 300-watt clamp-on electric heaters to the outside of a stainless steel tube (2.54 cm OD). The heaters are wrapped with 3.08 cm thick thermal insulation then covered by an aluminum outer shell. The heaters are spaced such that a higher heat flux is obtained in the boiling region with lower heat flux in the single-phase regions. The tube interior is filled with a copper foam material that reduces the flow perturbations and increases temperature uniformity in the boiling region. Three thermocouples are mounted to the outside wall of the boiler/superheater assembly. The superheater outlet temperature is feedback-controlled based on the desired superheater outlet temperature. Input power to the boiler section is set via computer and is not feedback controlled. The required boiler power is calculated via the data acquisition software based on the inlet water flow rate and temperature.

2.5 Operating conditions

Typical operating conditions for the 4 kW HTSE tests are listed in Table **II**. At the nominal operating conditions, the hydrogen production rate is 25 slpm or 1500 L/hr. This production rate is determined from the measurement of the electrical current supplied to the electrolysis cells using Faraday's law and is also independently verified based on the change in dew point values between the inlet and outlet dew point

sensors. The voltage and current across the electrolysis cell(s) is continuously monitored. Typical per-cell operating voltage will be 1.12 V.

3 Results

3.1 Preliminary test – two 10-cell stacks

A preliminary test using two 10-cell stacks was performed in the 4 kW test apparatus. The purpose of this test was to evaluate the functionality of all the components of the test apparatus, including gas supplies (H_2, N_2, air, steam), flow control, temperature control, heat recuperation, data acquisition and instrument control. The results would ensure that the 4 kW HTSE test stand would operate correctly in an integrated fashion. A photograph of the two 10-cell stacks installed in the test fixture is presented in Figure 7. The cells and stacks were subjected to the usual heatup and conditioning procedure, followed by initial DC potential sweeps and long-term operation of 100 hours duration. Figure 9 shows the stack voltage as a function of time over 100 hours of operation, indicating negligible performance degradation over this time period. As a conclusion, all the components of the test apparatus functioned properly and therefore were ready for the 4 kW HTSE tests.

3.2 4 kW HTSE test

For the 4 kW HTSE tests, two 40-cell stacks were installed in the test apparatus. A current density of 0.41 A/cm^2 was required in order to achieve 4 kW of electrolysis power. Operating conditions for this test are shown in Table **II**. The two 40-cell stacks installed in the test fixture are shown in Figure 9. Following stack installation, cell conditioning was performed over the next 54 hours. The process involved heating the stack initially to 600°C while purging with a mixture of 10% hydrogen and 90% nitrogen on the hydrogen electrode and with air flow on the oxygen electrode. Total flow rate on each side for this test was 55.5 slpm. The stacks were maintained at this condition for 20 hours. Subsequently, the stacks were heated up to 800°C, compressed to their final mechanical load of 1.78 kN, and maintained at this condition with the same flow rates and composition for another 24 hours. During the overnight period,

after heating to 800°C, there was a loss of nitrogen flow to the stack that lasted for a few hours. This event was caused by an incorrect level reading on a nitrogen Dewar due to a frozen float indicator. The stacks were consequently exposed to a low flow of pure hydrogen during this time. This event led to rapid reduction of the nickel oxide in the cell cathodes. This rapid reduction affected the bottom cell groups the most. These cell groups subsequently exhibited relatively high resistance because of rapid nickel metal grain growth. After completion of the 24 hour slow reduction process, the hydrogen mole fraction was then increased incrementally over the next 10 hours to achieve full reduction of the nickel oxide to nickel metal.

Initial performance characterization was achieved by executing individual DC potential sweeps for each stack, followed by an overall sweep for the two stacks operating in parallel. These sweeps were performed at a stack temperature of 780°C. Results of the individual stack sweeps are presented in Figure 10. The figures show the intermediate voltages of five cell groups with eight cells per group plus per-cell area-specific resistance (ASR) as a function of current density up to 0.42 A/cm^2. During the VI sweeps for Stack 1, the intermediate voltages for the three top cell groups exhibited very similar behavior. The highest voltages during the sweeps were observed for the bottom two cell groups, probably because of the rapid reduction event described earlier. The initial overall ASR for Stack 1 decreased with current density to a value of 0.86 Ω·cm^2 at 0.42 A/cm^2 . The sweep results for Stack 2 show that the intermediate voltages for the four top cell groups exhibited similar behavior. The highest voltages during the sweeps were observed for the bottom cell group, again probably because of the rapid reduction event described earlier. Voltages for the bottom cell group in Stack 2 were by far the highest of all the cell groups. The initial overall ASR for Stack 2 also decreased with current density to a value of 1.15 Ω·cm^2 at 0.42 A/cm^2.

Overall initial performance for the two stacks operating in parallel is shown in Figure 11, which includes stack voltage, per cell ASR, and electrolysis power as a function of current density. The overall stack voltage increased nearly linearly with current density to a maximum value of 53.3 V at 0.42 A/cm^2.

The initial overall ASR value was nearly independent of current density, with a value of 1.04 $\Omega \cdot cm^2$ at 0.42 A/cm^2. The corresponding total current was 0.84 A, with a total electrolysis power of 4.52 kW.

A long-term 4 kW HTSE stack test was performed after the initial performance sweeps. The furnace temperature was reduced to 750°C in order to avoid the possibility of overheating of the stacks. The results are shown in Figure 12, which depicts the time history of total current for the two stacks operating in parallel, the total electrolysis power, the stack voltage and the per cell ASR value. The initial current was ramped up from 40 A to 60 A over the first day of long-term testing to ensure all the components functioned correctly. Thereafter, the current were ramped up to 82 A. The stacks were controlled galvanostatically at a current density of 0.41 A/m^2, in order to maintain the electrolysis power just over the 4 kW level. The test duration target was 1000 hours operation at the 4 kW level.

Figure 12 shows the results for the first 920 hours of operation. Stack operation in the long-term mode was generally very stable, with no significant degradation in performance through 830 hours. The overall stack average ASR was 0.81 $\Omega \cdot cm^2$, which is an excellent value in the stack configuration, especially considering that the operating temperature was only 750 °C. The large fluctuations in the plotted values that began at 836 hours were related to a problem that developed with the deionized water delivery system. The pressure across the reverse osmosis (RO) device increased, resulting in a sudden loss of water flow delivery. The RO system was subsequently bypassed, but stable operation could not be fully restored.

The long-term behavior of the parallel stack intermediate voltages are plotted in Figure 13. The intermediate voltages were measured across eight consecutive cells, resulting in 5 voltage measurements for each stack. As mentioned previously, nitrogen flow loss affected the initial conditioning process. The intermediate voltages measured from the stacks clearly demonstrate that stack 2, especially the bottom 8 cells, suffered more from the interruption in nitrogen flow. Because of parallel operation, the stacks were compensating each other, so that the degradation cannot be evaluated individually for each stack.

4 Conclusion

A new test facility has been developed for multi-kW testing of HTSE stacks. This facility has provided a demonstration of HTSE operation at the 4 kW scale with advanced cell and stack technology. The 4 kW test included two stacks (40 cells per stack) operating in parallel in a single hot zone. The HTSE stacks were successfully operated for duration of 920 hours with low degradation. As a reference for future research, the factors used to design and develop multi-kW HTSE test facilities are provided. This successful large-scale demonstration of HTSE will help to advance the technology toward near-term commercialization.

5 Acknowledgement

This work was supported by the United States Department of Energy Office of Nuclear Energy, Very High Temperature Reactor Technology Development Office. Idaho National Laboratory is operated for the United States Department of Energy Office of Nuclear Energy by Battelle Energy Alliance, LLC, under contract No. DE AC07 05ID14517.

References

[1] C.M. Stoots, J.E. O'Brien, J.S. Herring, J.J. Hartvigsen, Journal of Fuel Cell Science and Technology, 6 (2009) 011014.
[2] S. Dillich, in: Annual Merit Review and Peer Evaluation Meeting, U.S. Department of Energy, 2014.
[3] R. Varrin, K. Reifsneider, D. Scott, P. Irving, G. Rolfson, Idaho National Laboratory, (2011).
[4] J.E. O'Brien, Journal of Heat Transfer, 134 (2012) 031017-031017.
[5] M.S. Sohal, J.E. O'Brien, C.M. Stoots, V.I. Sharma, B. Yildiz, A. Virkar, Journal of Fuel Cell Science and Technology, 9 (2012) 011017.
[6] J.E. O'Brien, 14th International Heat Transfer Conference, (2010).
[7] V. Utgikar, T. Thiesen, International Journal of Hydrogen Energy, 31 (2006) 939-944.
[8] W. Doenitz, R. Schmidberger, E. Steinheil, R. Streicher, International Journal of Hydrogen Energy, 5 (1980) 55-63.
[9] W. Doenitz, R. Schmidberger, International Journal of Hydrogen Energy, 7 (1982) 321-330.
[10] W. Doenitz, E. Erdle, International Journal of Hydrogen Energy, 10 (1985) 291-295.
[11] W. Doenitz, G. Dietrich, E. Erdle, R. Streicher, International journal of hydrogen energy, 13 (1988) 283-287.
[12] J. Herring, J. Obrien, C. Stoots, G. Hawkes, J. Hartvigsen, M. Shahnam, International Journal of Hydrogen Energy, 32 (2007) 440-450.
[13] C.M. Stoots, J.E. O'Brien, K.G. Condie, J.J. Hartvigsen, International Journal of Hydrogen Energy, 35 (2010) 4861-4870.
[14] X. Zhang, J.E. O'Brien, R.C. O'Brien, J.J. Hartvigsen, G. Tao, G.K. Housley, International Journal of Hydrogen Energy, 38 (2013) 20-28.
[15] G. Hawkes, J. O'Brien, C. Stoots, B. Hawkes, International Journal of Hydrogen Energy, 34 (2009) 4189-4197.
[16] A. Brisse, J. Schefold, Energy Procedia, 29 (2012) 53-63.
[17] S.D. Ebbesen, J. Høgh, K.A. Nielsen, J.U. Nielsen, M. Mogensen, International Journal of Hydrogen Energy, 36 (2011) 7363-7373.
[18] J. Mougin, A. Mansuy, A. Chatroux, G. Gousseau, M. Petitjean, M. Reytier, F. Mauvy, Fuel Cells, 13 (2013) 623-630.
[19] J. Mougin, A. Chatroux, K. Couturier, M. Petitjean, M. Reytier, G. Gousseau, F. Lefebvre-Joud, Energy Procedia, 29 (2012) 445-454.
[20] B. Yu, W. Zhang, J. Chen, J. Xu, S. Wang, Science in China Series B: Chemistry, 51 (2008) 289-304.
[21] Y. Bo, Z. Wenqiang, X. Jingming, C. Jing, International Journal of Hydrogen Energy, 35 (2010) 2829-2835.
[22] Q. Li, Y. Zheng, W. Guan, L. Jin, C. Xu, W.G. Wang, International Journal of Hydrogen Energy, 39 (2014) 10833-10842.
[23] Y. Zheng, Q. Li, W. Guan, C. Xu, W. Wu, W.G. Wang, Ceramics International, 40 (2014) 5801-5809.
[24] S.-D. Kim, J.-H. Yu, D.-W. Seo, I.-S. Han, S.-K. Woo, International Journal of Hydrogen Energy, 37 (2012) 78-83.
[25] J. Hong, H.-J. Kim, S.-Y. Park, J.-H. Lee, S.-B. Park, J.-H. Lee, B.-K. Kim, H.-J. Je, J.Y. Kim, K.J. Yoon, International Journal of Hydrogen Energy, (2014).

Table I. Design factors of multi-KW high temperature steam electrolysis experiments.

Design Factor	Description	Specs used in this research
Power requirement	• Determine the specifications of the DC power supply needed for multi-KW HTSE test. • Determine the AC power supplies for the steam generator, heat traces, and the furnace. • Ensure the circuit breakers, power plugs and sockets are in compliance with the specifications of the power suppliers.	DC power supply: TDK-Lambda Gen 100-100; 3-phase 208 V input. Furnace: Applied Test Systems Series 3210, 15 KW, 208 V, 3-phase power input. Heat trace power control: Watlow Din-a Mites, 110 V input. Steam generator: Watlow clamp heater, 240 V input.
Gas supplies and distribution	• Determine the gas consumption rates so that the gas sources can be specified. Normally gases are supplied from compressed bottles, gas generators, or cryogenic Dewar. • Design a manifold that distribute the gas flows to and from the stacks.	H_2: compressed bottles and H_2 generator. N_2: Dewar. Air: air compressor.
Steam generation	• Determine method for steam generation based on the steam content in the feedstock. Steam can be produce using either a humidifier or a steam generator.	Steam is produced from a homemade steam generator.
Piping	• Determine the tubing dimension and ensure no turbulent flow will occur. • Determine the materials of tubing according to their environmental temperature. • Determine the length of tubing needed for preheating.	Tubing dimension: 12.7 mm OD × 0.899 mm Wall. Materials: stainless steel (304) for temperature < 500 °C; Inconel for temperature > 500 °C.
Heat recuperation	• Calculate the preheating requirement for the inlet gases and design (or select) heat exchangers accordingly.	Tube-in-tube (Inconel inside and stainless steel outside) heat exchangers for preheating and cooling. Coiled Inconel tubing for further preheating.
Data acquisition (DAQ)	• Acquire a DAQ system with enough channels for collecting data (temperature, voltage, current, pressure, etc.).	Agilent DAQ system.
Safety	• Setup a gas alarm system for emergency shutdown. • Setup independent overtemperature protection for all the heating elements controlled by the computer. • Insulate high voltage DC terminals.	Gas monitor: Draegergard CCS 3000 to monitor CO, CO_2, H_2, and O_2. Overtemperature protection: usually 20-50 °C above the setting points.

Table II. Operating conditions for 4 kW HTSE test (80 cells).

Electrolysis power input (kW)	4.01
Stack current (parallel double stacks) (A)	82
Current density (A/cm^2)	0.41
Stack voltage (V)	48.9
Stack temperature (°C)	750
Stack pressure	ambient
Gas flow rates (slpm)	
▪ Inlet hydrogen	14.9
▪ Hydrogen production rate	23.4
▪ Inlet steam	52
▪ Inlet nitrogen	7.4
▪ Sweep air	70
Steam utilization (%)	45
Inlet steam mole fraction	0.70
Inlet hydrogen mole fraction	0.20
Inlet nitrogen mole fraction	0.10

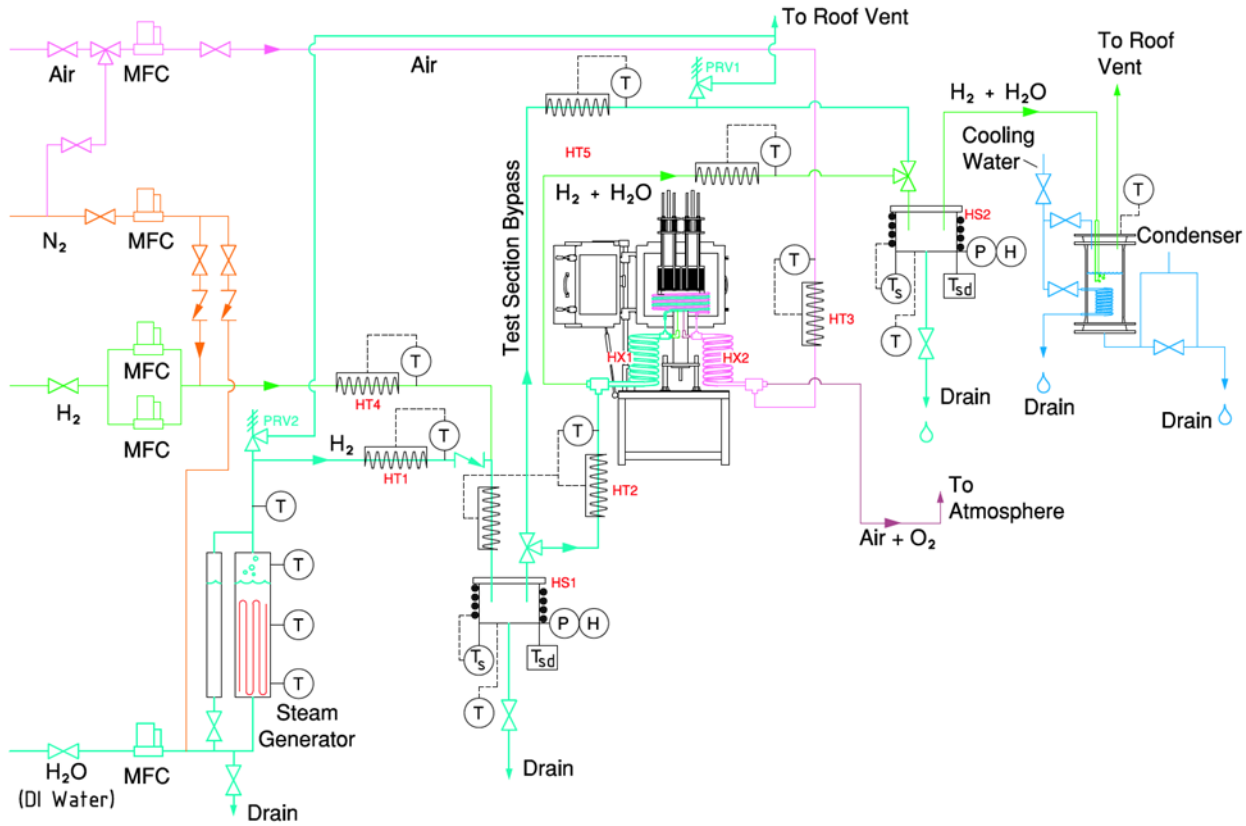

Figure 1. 4 KW high temperature steam electrolysis P&ID.

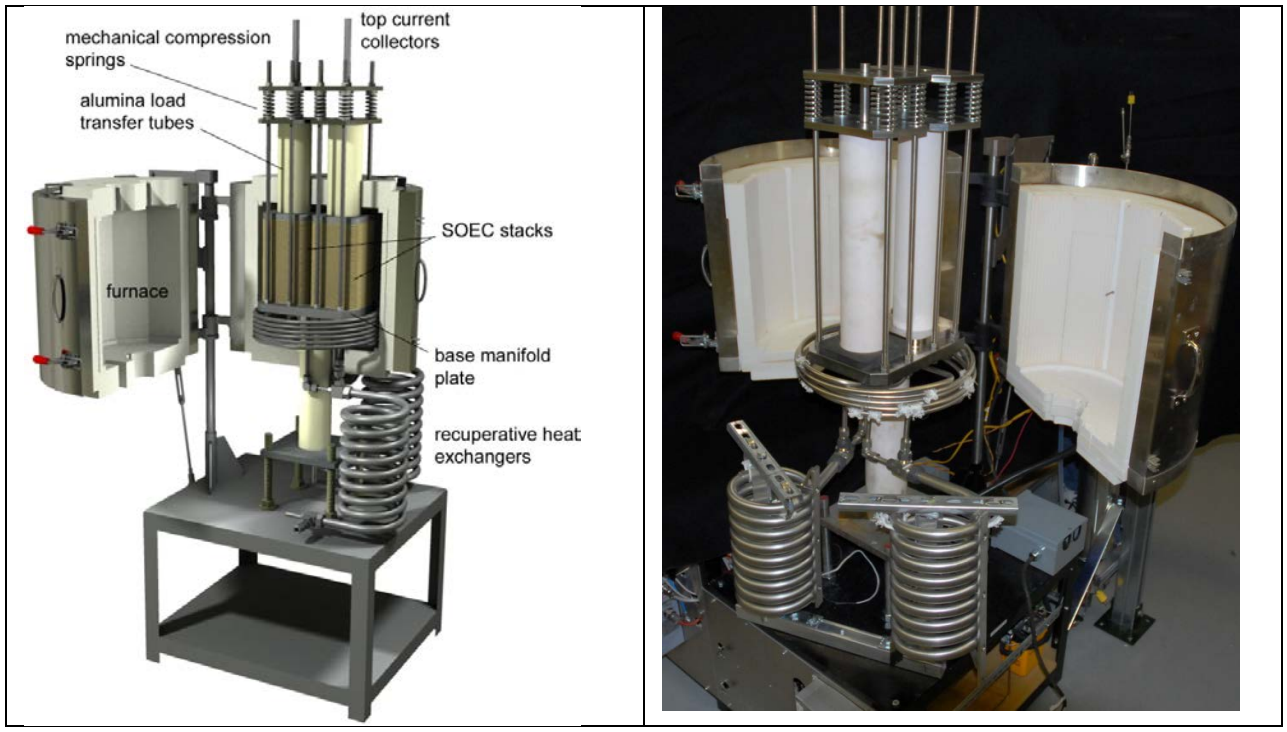

Figure 2. 4 KW test stand. a) 3D CAD design; b) actual test stand prior to the tests (without SOEC stacks).

Figure 3. Base manifold plate and coiled tubing, (a) top, (b) bottom.

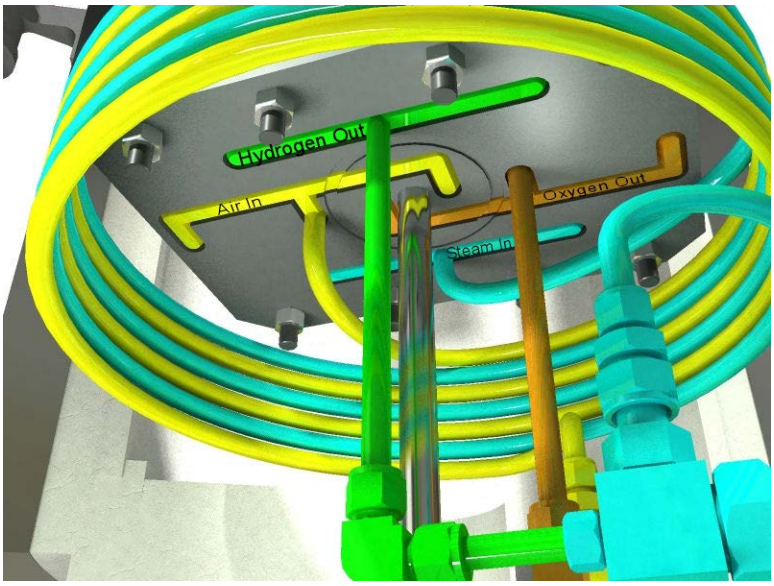

Figure 4. Color-coded rendering of the base manifold plate showing the inlet and outlet gas flow lines and seal-welded flow channels.

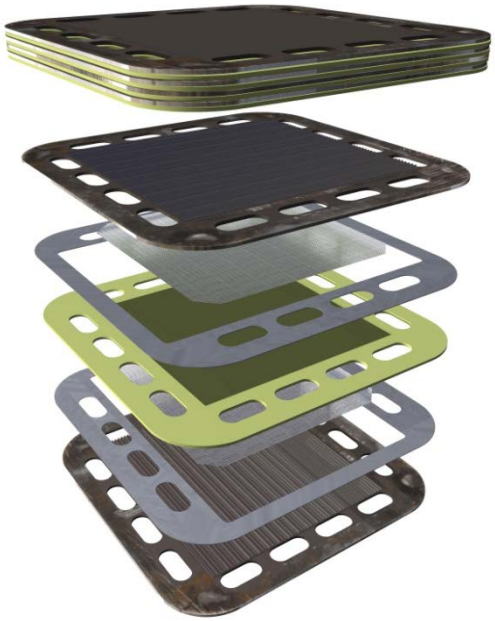

Figure 5. An exploded view of an assembly unit of the SOEC stack made by MSRI.

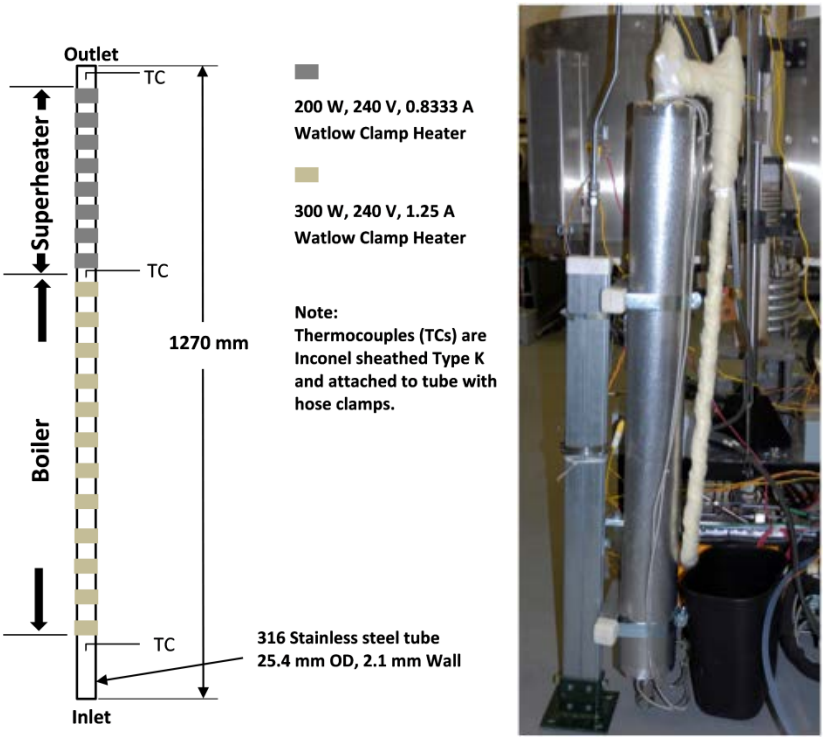

Figure 6. Schematic of custom steam generator and the actual steam generator next to the test stand.

Figure 7. Two 10-cell stacks installed in the 4 kW test fixture, ready for the preliminary test.

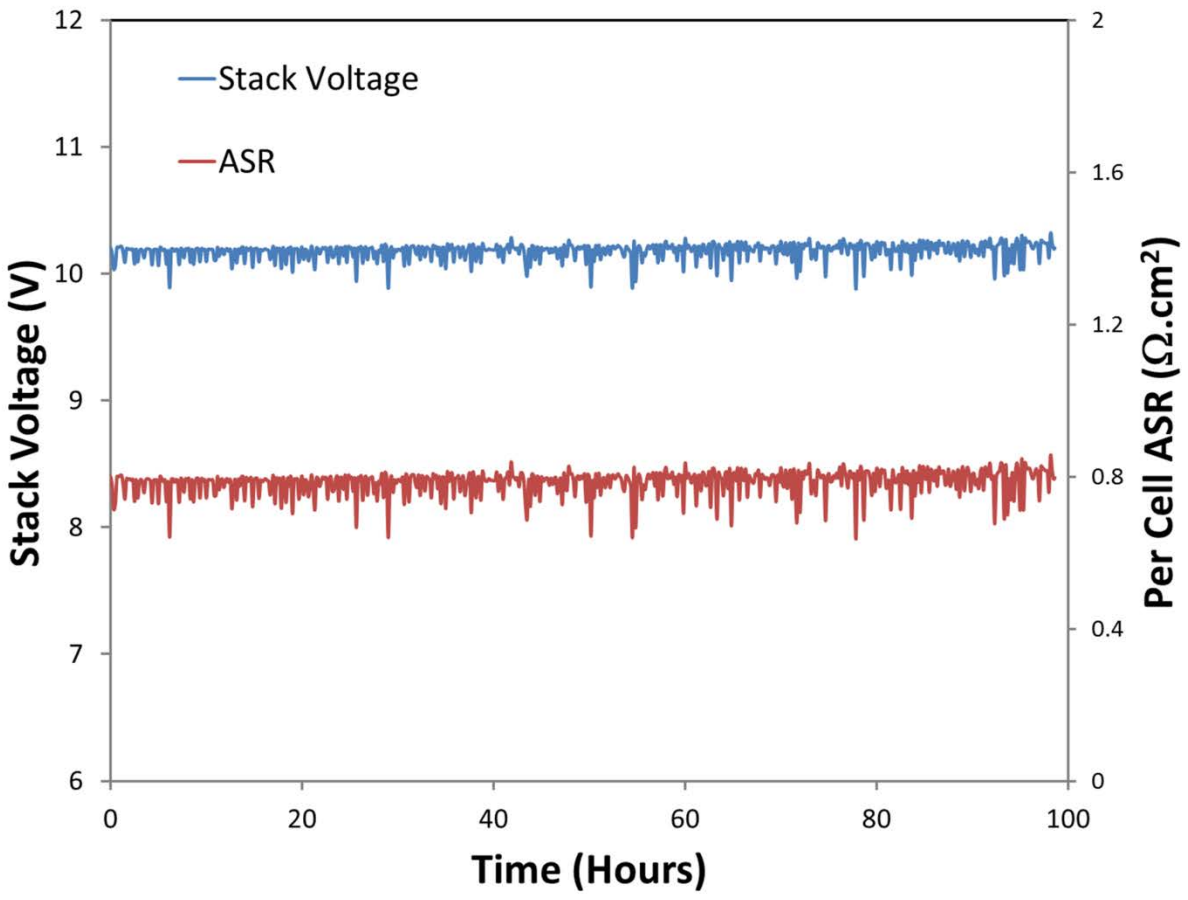

Figure 8. HTSE 100-hour preliminary test using two 10-cell stacks.

Figure 9. Two 40-cell stacks installed in the test apparatus.

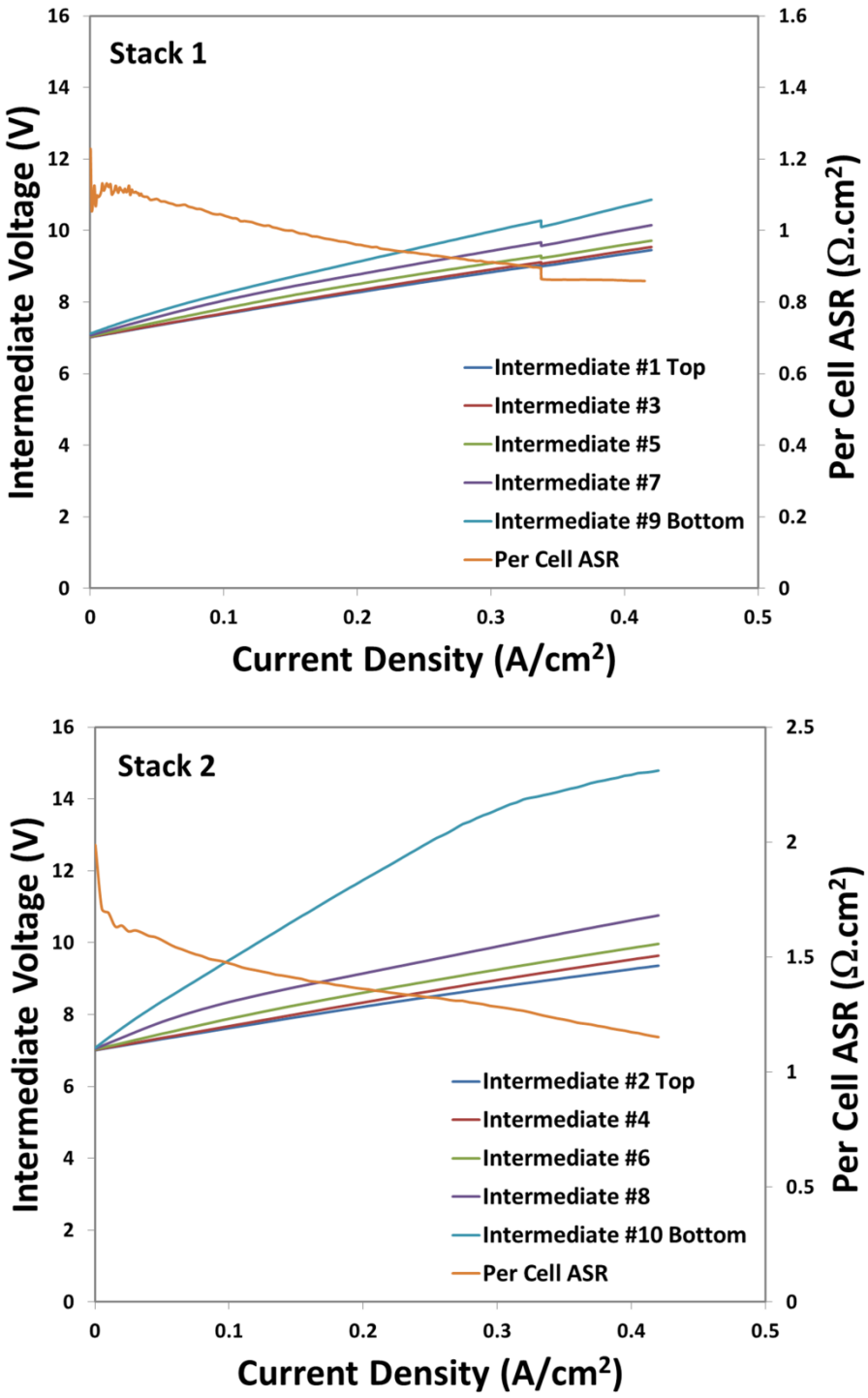

Figure 10. Initial VI sweeps of stack 1 and 2. The intermediate voltages were measured the voltage across 8 cells (shown in Figure 9).

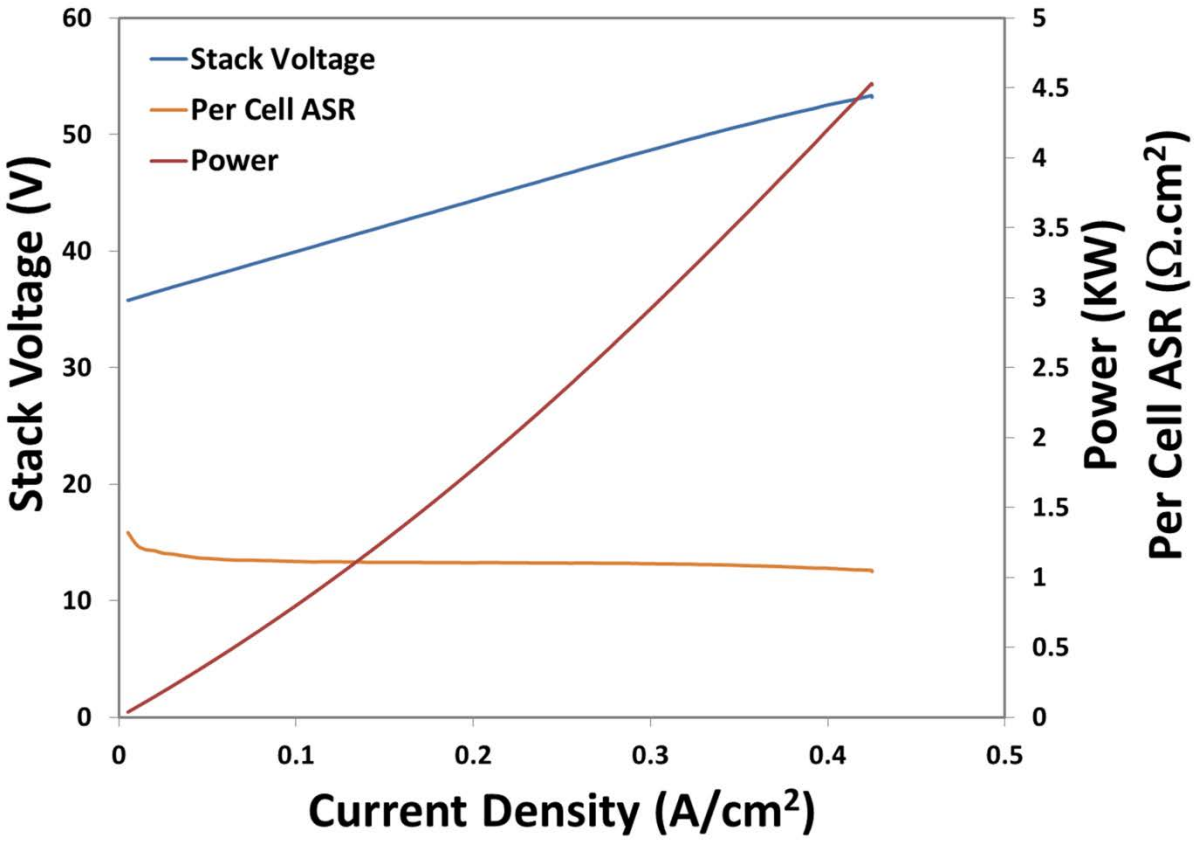

Figure 11. Initial performance of two 40-cell stacks operating in parallel.

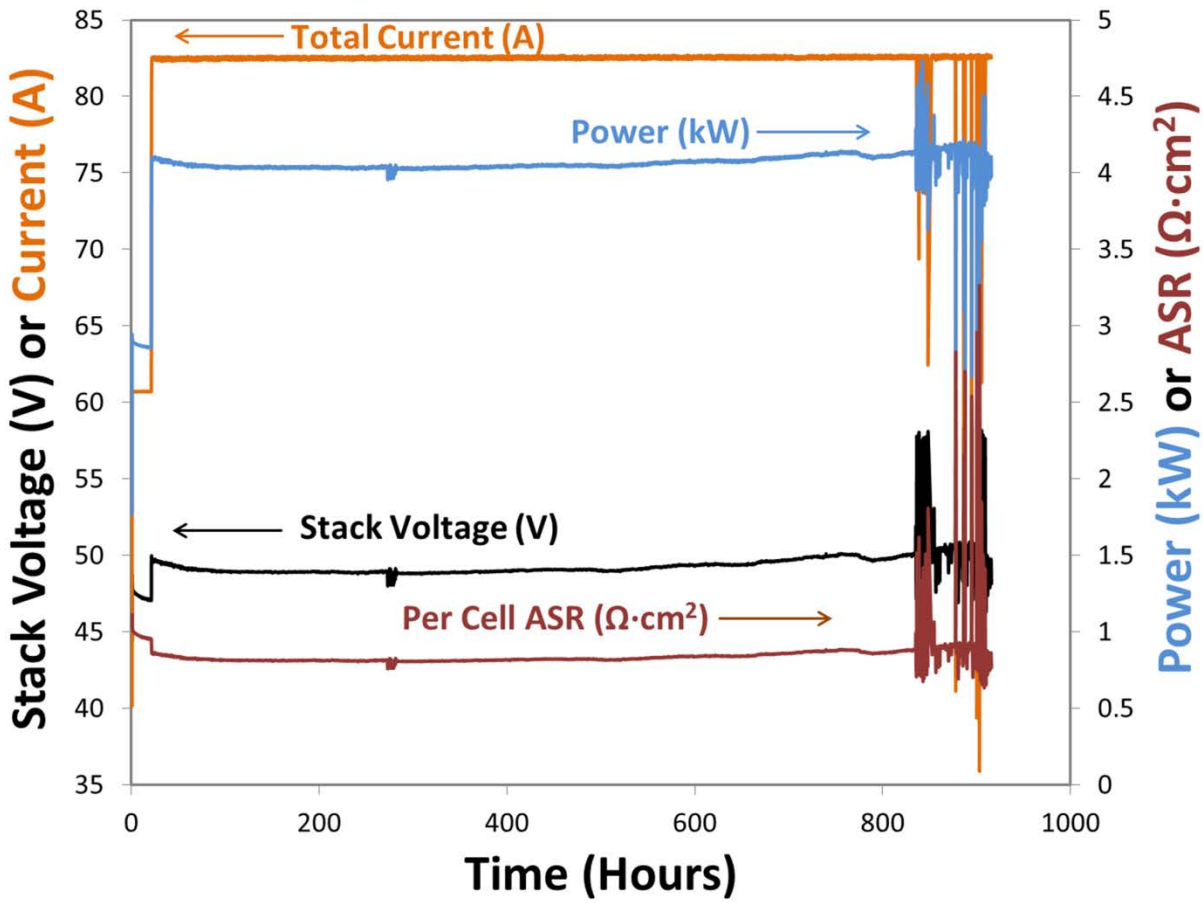

Figure 12. Long-term 4 kW HTSE test results through 920 hours of operation.

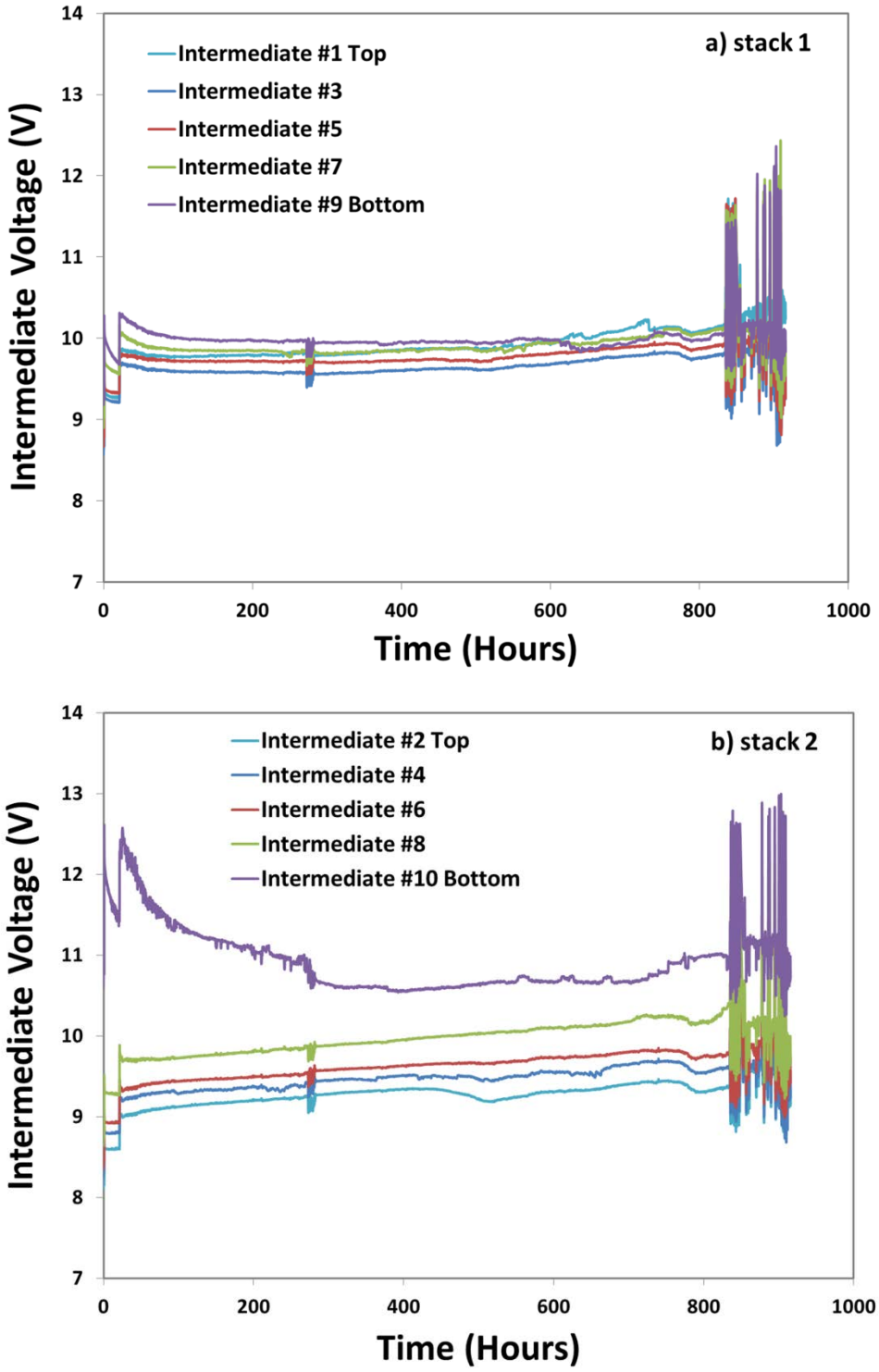

Figure 13. Intermediate voltages of a) stack 1 and b) stack 2 during 920 hours operation. The intermediate voltages were measured the voltages across 8 consecutive cells.